

A methodology to quantify debris generation after a seismic event

Original

A methodology to quantify debris generation after a seismic event / Domaneschi, Marco; Scutiero, Gianluca; Marasco, Sebastiano; Cimellaro, GIAN PAOLO; Amir KHALIL, Ahmed; Pellecchia, Cosimo; DE IULIIS, Emiliano. - ELETTRONICO. - 1:(2018). (Intervento presentato al convegno 16th European Conference on Earthquake Engineering (16ECEE) tenutosi a Thessaloniki nel 18-21 June 2018).

Availability:

This version is available at: 11583/2724253 since: 2019-01-31T00:24:38Z

Publisher:

Curran Associates, Inc

Published

DOI:

Terms of use:

This article is made available under terms and conditions as specified in the corresponding bibliographic description in the repository

Publisher copyright

(Article begins on next page)

A METHODOLOGY TO QUANTIFY DEBRIS GENERATION AFTER A SEISMIC EVENT

Marco DOMANESCHI¹, Gianluca SCUTIERO¹, Sebastiano MARASCO¹, Gian Paolo CIMELLARO¹, Ahmed Amir KHALIL², Cosimo PELLECCIA³, Emiliano DE IULIIS³

ABSTRACT

Seismic damage simulation at the regional scale can potentially provide valuable information that can facilitate decision making, enhance planning for disaster mitigation, and reduce human and economic losses. When an earthquake happens, building damage assessment is one of the important issues in earthquake loss estimation. The amount of debris generated and the effects on related critical infrastructures is also an essential information to evaluate. Indeed, as cascading consequence of debris accumulation, the road network can be interrupted. This entails an overall increase in the average number of people who have difficulty evacuating, with high risk that residents cannot evacuate any areas. This study proposes a method to evaluate the debris affected area and the debris amount as a function of the geometric characteristics and the level of damage of the buildings. The first part of this work is focused on the evaluation of the debris area's extension by numerical simulations. Comparison of the results with images of real seismic damaged structures allows the validation of the results. Besides, experimental tests on a small shaking table are performed to validate the numerical simulations. A mathematic model based on the results is also proposed.

Keywords: Earthquake; Debris; Applied element method; Masonry building; Collapse;

1. INTRODUCTION

In recent years, seismic events hit several territories such as the center of Italy (2016) and Mexico (2017). In order to reduce the social and economic losses, the emphasis has shifted to mitigations and preventive actions before the earthquake events (Cimellaro 2016). Large amounts of debris may be generated after a seismic event due to the buildings collapses and could constitute a serious obstacle to the escape routes. This entails an overall increase in the average number of people who have difficulty evacuating. The generation of debris due to earthquakes has been studied by some authors. For example, S. García-Torres et al. (2017) or Rafee et al. (2008) analyzed the implementation of strategies in debris management after seismic events. By a material stock analysis Tanikawa et al. (2014) examined the losses of building and infrastructure materials after disasters such as a tsunami or an earthquake. No methodology to quantify the extension area within which debris fall was developed in order to determine whether a road is blocked or not. This work proposes a methodology to estimate this area by the development of collapse scenarios of buildings. The research has been focused on masonry buildings; they represent much of the Italian cultural heritage and most of the European historic buildings. This paper is divided into two sections. The first section provides a description of the proposed methodological approach. In the second section the main findings are discussed and the conclusions of this work are presented.

¹Department of Structural, Geotechnical & Building Engineering (DISEG), Politecnico di Torino, ITALY
marco.domaneschi@polito.it

²Applied Science International, LLC, USA, khalilaa@appliedscienceint.com

³ASI Europe SRL, Italy, cpellecchia@appliedscienceint.com

2. METHODOLOGY

2.1 Applied Element Method

The proposed methodology in this study is based on the correlation between geometric parameters of the building and the debris area. For this research an Applied Elements Method (AEM) based software is used. The AEM is an innovative modeling method adopting the concept of discrete cracking. Through two decades of continuous development, AEM was proven to be the method that can track the structural collapse behavior passing through all stages of the application of loads: elastic stage, crack initiation and propagation in tension-weak materials, reinforcement yielding, element separation, element collision (contact), and collision with the ground and with adjacent structures. Although the FEM is accurate and reliable for analysis of continuum structures, the onset of element separation is difficult to automate and modeling of debris collision is time consuming. With AEM, the structure is modeled as an assembly of small elements, which are made by dividing the structure virtually, as shown in Figure 1. The two elements shown in Figure 1 are assumed to be connected by one normal and two shear springs located at contact points, which are distributed around the elements' edges. Each group of springs completely represents stresses and deformations of a certain volume as shown in Figure 1.

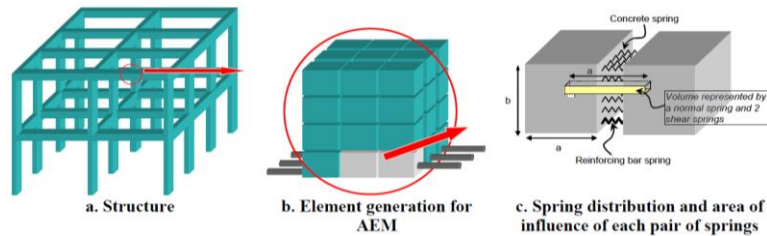


Figure 1. Modeling of structure to AEM

These springs reflect the different material properties; strain stresses and failure criteria are all calculated and estimated using these springs.

2.2 AEM for Masonry Building

Using AEM method, the brick can be simulated either in a staggered pattern, in its real configuration, or as homogenous material as shown in Figure 2. The real configuration includes the individual bricks in a staggered pattern connected by interface springs with mortar by material properties. The brick itself can be divided into sub-elements to allow the cracks to develop inside an individual brick. Since it is not practical to model the mortar as separate elements, the thickness of mortar is not included in the real configuration approach. On the other hand, the continuum simulation, or the macro simulation, represents the brick wall as one homogenous material. Instead, average properties should be introduced by the user for the mortar and the adjacent brick element. The reinforcing steel bars are modeled by springs that represent the material properties, exact location and dimensions of the bars. The generation of these springs is automatically performed in the software Extreme Loading for Structure.

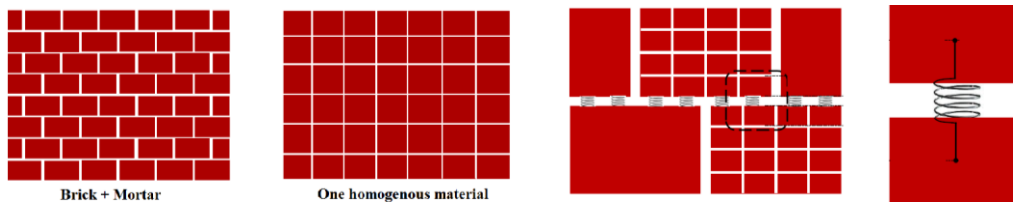


Figure 2. Different meshing for masonry

2.3 Case study: shaking test

A case study conducted by Imai H. et al. (2015) on masonry buildings subjected to earthquake with a shaking table is considered to evaluate the accuracy of a simulation by AEM method and the influence of mesh discretization on the solution. Two houses were built and dynamically tested with fourteen input motions on a seismic simulator at National Research Institute for Earth Science and Disaster Prevention (NIED) on February 23-24, 2011. Buildings views are shown in Figure 3.

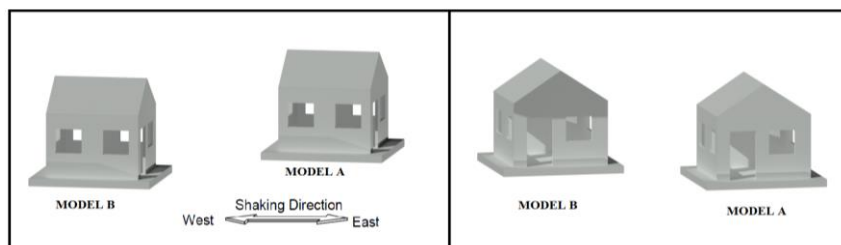


Figure 3. Isometric views of two models on shaking table

Model A is constructed with the flowing materials, in compliance to the minimum requirements set in the National Structural Code of the Philippines (NSCP2010). The walls are made of 400 mm x 200 mm x 150 mm concrete hollow blocks (CHB). The mortar mix used for filling and joint mortar is properly compacted. The vertical and horizontal reinforcement bars used are 10 mm and are spaced at 400 mm and 600 mm respectively. Model B represents the non-engineered construction of typical houses in Philippines; It is made of 400 mm x 200 mm x 100 mm CHB and filled hollows and joints with mortar having a mix ration of 1:4 (by volume of cement and sand). The reinforcement used size of 6 mm diameter and is spaced at 600 mm along the horizontal direction and at 900 mm along longitudinal direction. Compression strength tests were performed on prism specimens of masonry unit of concrete hollow blocks (Figure 4) at Mie University (Japan). Vertical reinforcing bars were not installed. Tests shows that the compressive strength of the mortar used for the prism specimens ranges from 9.5 N/mm² to 15.2 N/mm². In the table 1 and 2 the results are shown.

Table 1. Prism specimens of concrete hollow blocks (CHB).

	CHB	Reinforcing bar	Mortar	
	Thickness		Mixing ratio	Compaction
Specimen D	6 inch, 150 mm	None	1 cement : 4 sand	Compacted
Specimen E	6 inch, 150 mm	None	1 cement : 4 sand	Not Compacted
Specimen F	4 inch, 100 mm	None	1 cement : 4 sand	Compacted

Table 2. Prism compressive strength.

	[N/mm ²]
Specimen D	4.40
Specimen E	1.42
Specimen F	2.52

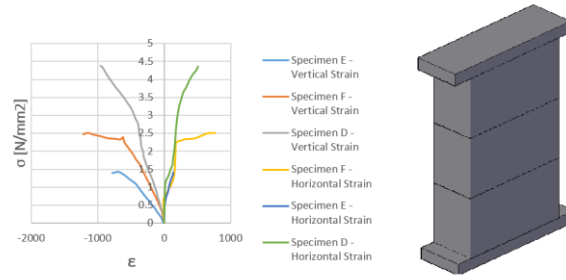


Figure 4. Compressive test results

Only model B is modeled by AEM software like homogeneous material. As can be seen in Table 1, the test show that for Philippine CHB masonry structures, the application of mortar is a critical and important aspect of construction because the CHB itself has a poor strength. Tested material specimens reported in Figure 4 and Table 1 do not include that one of Model B. Indeed, CHBs thickness of building Model B (100 mm) is smaller than material specimen E (150 mm in Table 1). Consequently, the mechanical properties of specimen E are higher than Model B. Therefore, to validate AEM model with the performed shaking table tests, the material parameters are decreased until the partial collapse at the top of gable wall during input motion # 7 is equivalent to that recorded during the laboratory test. The same seismic inputs of the shaking table tests have been used for the numerical simulations with the AEM. They are reported in Figure 5. The damages caused by the shaking test are reported in Table 3.

Table 3. Damage status of the model structure at main inputs.

February 24, 2011	PGA	Damage status
No.7	0.85 g	East wall: Gable wall collapsed (fell). Upper part of opening had large displacement. West wall: Gable and upper part of wall was collapsed (fell). North and South wall: Minor cracks
No.12	1 g	East and West walls were collapsed, then this model was totally collapsed.

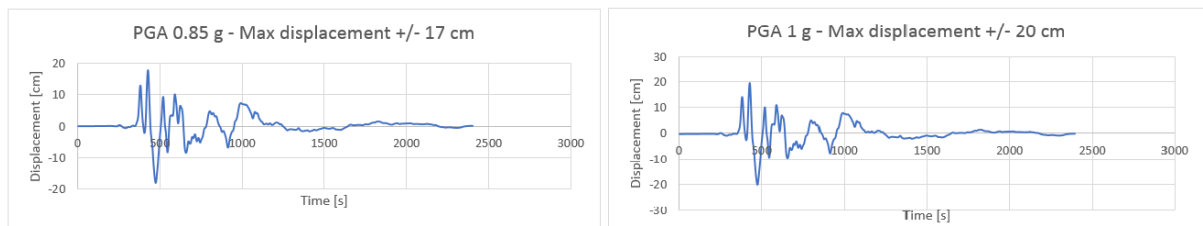


Figure 5. Input motion n°7 and n°12

In Table 4, the mechanical parameters of AEM model are shown. Where f_m is the compressive strength, f_{vk} is the shear strength, E is the elastic modulus and G is the shear modulus.

Table 4. Input mechanical parameter for AEM model.

f_m [N/mm ²]	f_{vk} [N/mm ²]	E [N/mm ²]	G [N/mm ²]
1.15	0.35	24000	6000

In Figure 6 a graphical output compared with the real picture is done while in the Figure 7 the AEM

displacements with the displacements obtained by shaking test are compared.

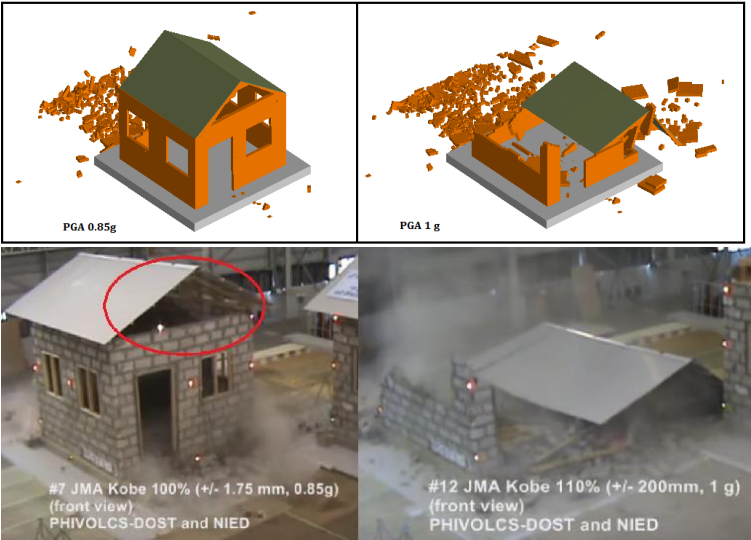


Figure 6. Compare between real model B and AEM model

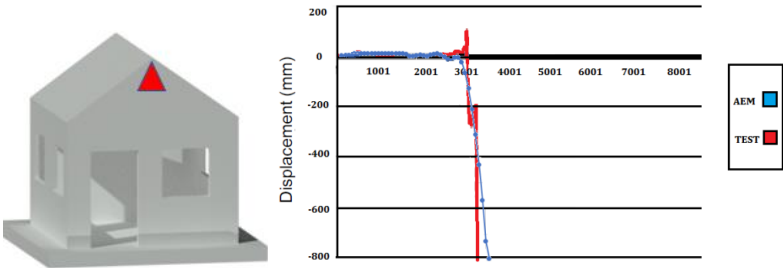


Figure 7. Displacement data of top of gable walls during input No. 7

In order to evaluate the influence of mesh discretization on the solution, a sensitivity analysis is performed. The number of mesh has been decreased until the displacement of top of gable walls has shown further significant changes. As reported in Figure 8, at the decreasing of elements number correspond an increase of the resistance to the collapse.





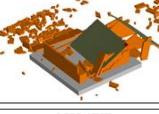
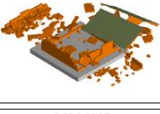




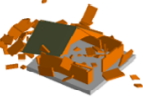

NAME	MESH AEM MODEL	PGA	COLLAPSE	NAME	MESH AEM MODEL	PGA	COLLAPSE
Mesh 1		0.85g		Mesh 2		0.85g	
		1 g				1 g	
NAME	MESH AEM MODEL	PGA	COLLAPSE	NAME	MESH AEM MODEL	PGA	COLLAPSE
Mesh 3		0.85g		Mesh 4		0.85g	
		1 g				1 g	

Figure 8. Different meshing of AEM model

For a number of elements equal to Mesh 2, the results tend to be acceptable, as shown in Figure 9. The results of “mesh 3” and “mesh 4” have not been represented in the chart, because the displacements of the considered element are very far from the exact solution.

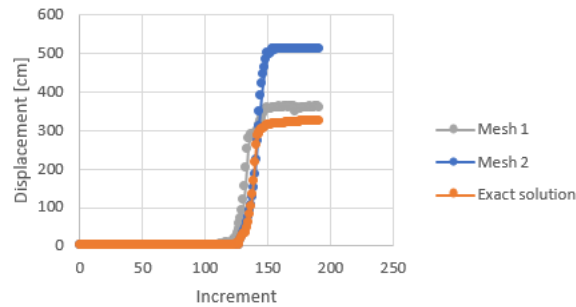


Figure 9. Displacement of top of gable walls for different meshing levels

Therefore, the solution “mesh 2” is chosen for the analysis. Walls were discretized with 13 elements on the short side of the building, 15 elements on the long side and one element along the thickness. It can be asserted that the AEM analysis shows a good accordance with the real test. Therefore, the time-step and mesh discretization settings used for the Philippine CHB building is maintained for further analysis to estimate debris areas of masonry buildings.

2.3 Debris Area

Numerical simulations are performed on 27 types of buildings groups. Each group consists of three types of building with 1, 2 and 3 floors respectively, leading to a total of eighty one models. The sides' dimension and the area of the rectangular footprint for each group of three buildings are shown in Table 5.

By a nonlinear dynamic analysis, for each building a progressive collapse is simulated. The Central Italy 24/08/2016 earthquake record is used for the analysis. As shown in Figure 10, the earthquake is applied in four different directions rotated by 45 degrees around the vertical axis; Therefore, four collapse simulations for each case study are available. That one with the largest debris area is only considered.

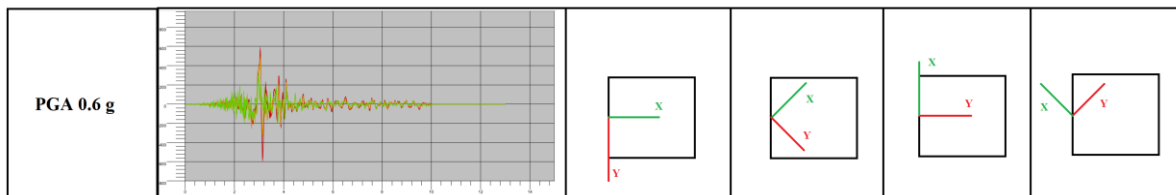


Figure 10. Accelerogram and earthquake directions.

Mechanical parameters are calibrated accordingly with the current Italian standard on existing masonry (NTC 2008), as homogenous material. To amplify the area of debris, the masonry typology with the lowest mechanical parameters are used, as shown in Table 6.

In Figure 11, a sample of full collapse performed by AEM software is shown.

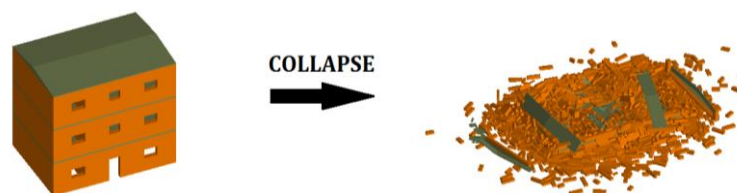


Figure 11. Example of AEM simulation

A scale factor to enlarge the building's footprint is considered for including the debris. The area may be much larger than the required area (Figure 12). This error is due to maintain the building's sides ratio constant.

Table 5. Group analyzed.

Group	Ratio	a[m]	b[m]	Area [m2]
1	0.2	4	20	80
2	0.3	4.9	16.3	79.9
3	0.4	5.7	14.1	80.4
4	0.5	6.3	12.6	79.4
5	0.6	6.9	11.5	79.4
6	0.7	7.5	10.7	80.3
7	0.8	8	10	80
8	0.9	8.5	9.4	79.9
9	1	8.9	8.9	79.2
10	0.2	8	40	320.0
11	0.3	9.8	32.6	319.5
12	0.4	11.4	28.2	321.5
13	0.5	12.6	25.2	317.5
14	0.6	13.8	23	317.4
15	0.7	15	21.4	321.0
16	0.8	16	20	320.0
17	0.9	17	18.8	319.6
18	1	17.8	17.8	316.8
19	0.2	12	60	720.0
20	0.3	14.7	48.9	718.8
21	0.4	17.1	42.3	723.3
22	0.5	18.9	37.8	714.4
23	0.6	20.7	34.5	714.2
24	0.7	22.5	32.1	722.3
25	0.8	24	30	720.0
26	0.9	25.5	28.2	719.1
27	1	26.7	26.7	712.9

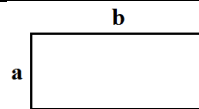


Table 6. Mechanical parameters used (NTC2008).

f_m [N/mm2]	f_{vk} [N/mm2]	E [N/mm2]	G [N/mm2]
1.0	0.2	690	230

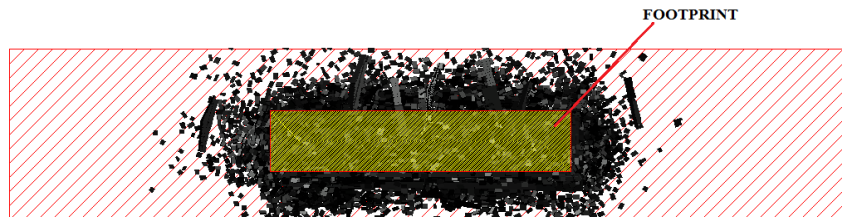


Figure 12. Footprint area vs scale factor area

As shown in Figure 13, a central area with a major debris presence and an outer area with a smaller amount. By neglecting a low percentage of debris, it is possible a new rectangular high debris density area can be defined (in red in Figure 15).

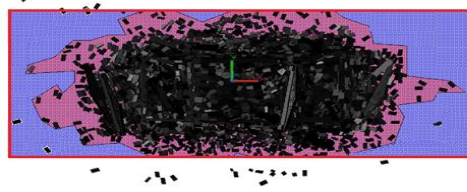


Figure 13. Scale factor area with neglecting percentage of debris

By a Cad software the AEM output file can imported and the coordinates of the debris amount can be saved in a text file. This last can be easily uploaded in Matlab environment for further evaluations. Coordinates of all points into the file are exported in txt format. The code has two functions:

- A rectangular area with a percentage of internal points can be defined through a scale factor (Figure 14);
- Another area that contain all the debris can also be identifies through a polyline (Figure 14).

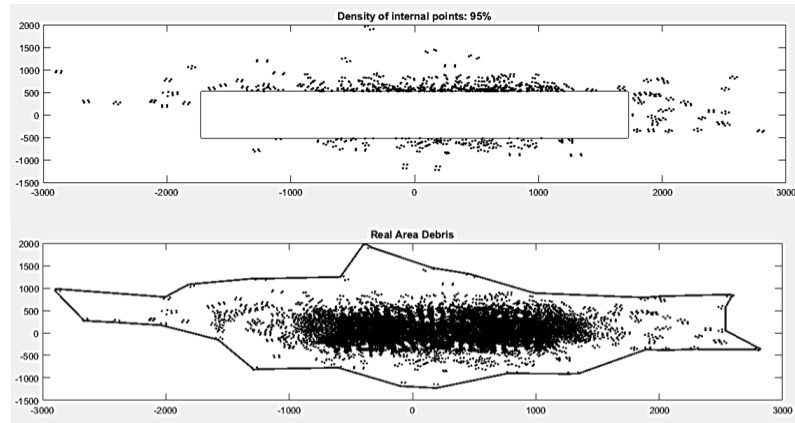


Figure 14. Scaled rectangular area with a given percentage of internal points and Real area of debris bounded by a polygonal

As shown in Figure 15, other two geometries (elliptic and circular) are considered and compared with rectangular shape. The ellipse axes and the circle radius are scaled with the same principle as the rectangle (scale factor).

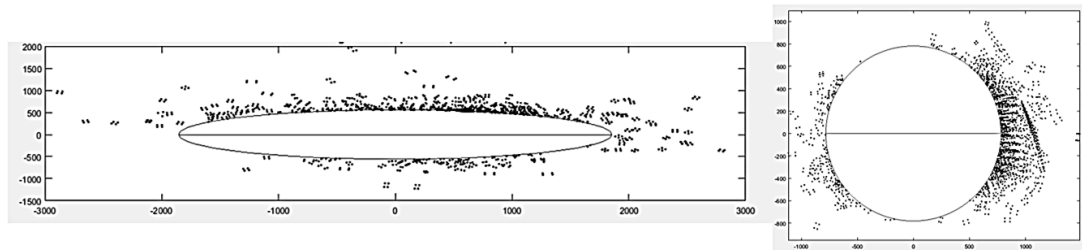


Figure 15. Ellipse and circle area

In function of the building's area different cases of percentage of inside points in function of the building's area are considered as shown in Table 7.

Table 7. Percentages of inside points considered.

	1 floor	2 floors	3 floors
	100%	100%	100%
\Area: 80 m2	90%	90%	95%
	80%	80%	92.50%
	70%	70%	90%
Area: 320 m2	100%	100%	100%
	95%	97.50%	98%
	90%	95%	96%
	80%	92.50%	94%
Area: 720 m2	100%	100%	100%
	97.50%	98.80%	99.30%
	95%	97.60%	98.60%
	92.50%	96.40%	97.90%

To every percentage of neglected points corresponds a volume of debris.

2.4 Road interruption simulation

In order to evaluate the amount of debris that can be able to interrupt a standard road an AEM simulation is performed and the volume limit for passing a vehicle is calculated. According to Italian road regulations (art. 2, Decreto Legislativo 30 aprile 1992, n. 285), a 3,5-meter road with a 0,50-meter sidewalk and the axles of the vehicle are modeled. The presence of debris on a road surface whose distribution derives from the simulation carried out for a 3-storey building with a ratio of 1 is performed. The test is passed if the vehicle starting from point A can reach point B. Four scenarios with different debris volumes are simulated: 25 cubic meters, 20 mc, 15 mc, 10 mc (Figure 16).

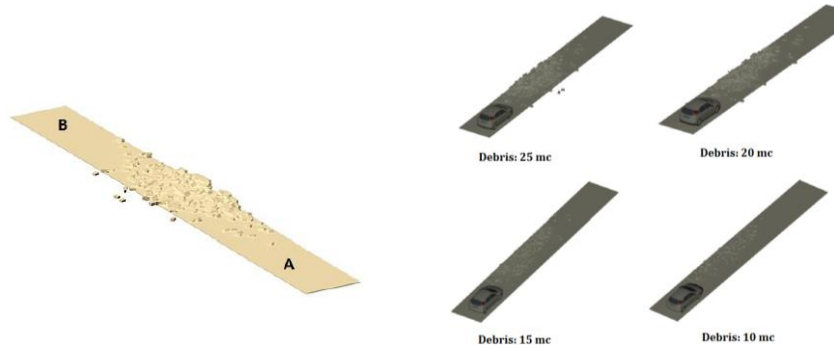


Figure 16. Simulation car for different volumes of debris

The total weight (1300 Kg) of the vehicle is distributed on the four tires. The dimensions of the car considered are shown in figure 17.

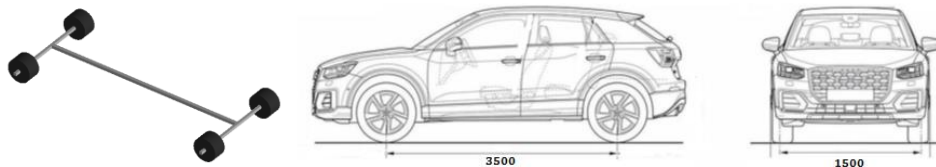


Figure 17. Car AEM model and dimensions

The vehicle is modeled like a rigid body. The car body was neglected for two reasons:

- 1) To reduce the computational efforts;

- 2) As the simulation performed represents an emergency, it is assumed that it is not priority to evaluate the car body.

The model of the tire is 225/45 R17. To each tire is assigned a rotation of 2 of a lap per second (10 km/h). Uniform motion in a straight line is assigned to the car. The vehicle moves along the road, it can change its direction only because of an obstacle. In Table 8 the results are shown.

Table 8. Car test results.

Test	Volume	Result
1	10 m3	Passed
2	15 m3	Passed
3	20 m3	Not Passed
4	25 m3	Not Passed

2.5 Results

Referring to Table 6 and taking in account also the results obtained in paragraph 2.4, the difference of the measured area with the real one (error) for the different percentages are analyzed. The combinations “debris volume passed by car test-error” with the lowest values are considered, as shown in Table 9. These percentages correspond to a neglected debris volume between 11 and 14 cubic meters. As the volume of the building grows, the outer area with less debris is less extensive as shown in Figure 18.

Table 9. Percentage of inside points.

	1 floor	2 floors	3 floors
80 m2	80%	90%	92.5%
320 m2	95%	97.5%	98%
720 m2	97.5%	98.8%	99.30%

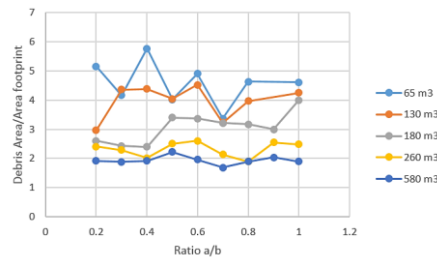


Figure 18. Debris Area/Outer debris volume - ratio

Rectangular geometry has been selected as the best performer with respect to circular and ellipse area. For the circle the error is higher for low ratios, but decreases for unitary ratios. In the figure 19, the results are shown and only the values of scale factors obtained by rectangular shapes are considered.

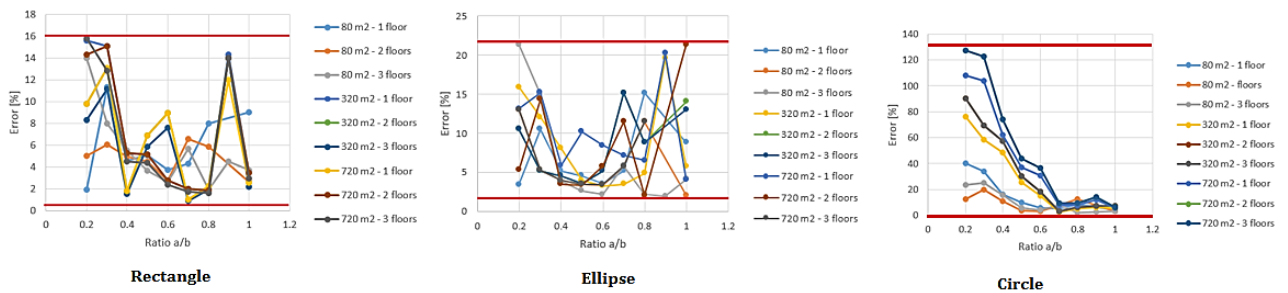


Figure 19. Error – ratio a/b

The data are interpolated through a plan as shown in Figure 20-a. Two residuals tests are performed to verify the reliability of the model. The normality of the residuals is validated by Shapiro-Wilk test that confirm the normality hypothesis as shown in Figure 20-b. In the second test the predicted residuals are compared with predicted values to validate the homoscedasticity hypothesis. As shown in Figure 20-c it is satisfied.

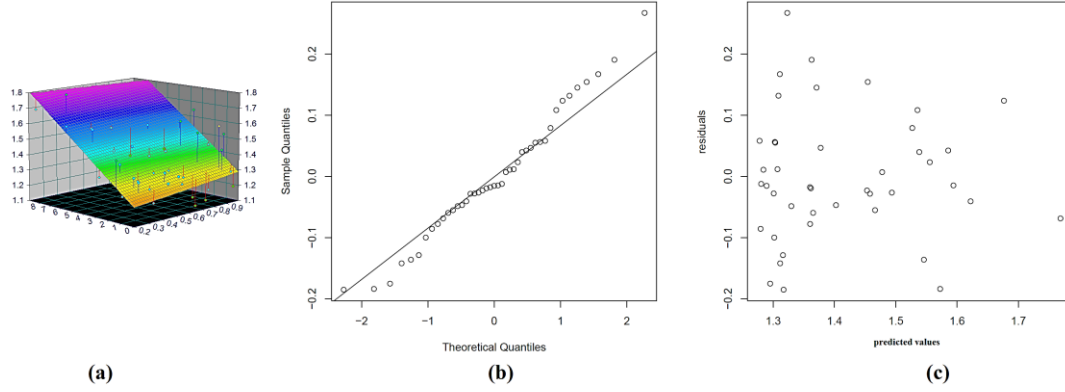


Figure 20. Residuals chart

The formula for obtaining rectangular shape scale factor is given by:

$$scale\ factor = 1.202 + 0.0864 \cdot \left(\frac{a}{b}\right) + 0.0659 \cdot \left(\frac{Area_{footprint}}{Volume_{building}} \cdot \frac{h_{building}^2}{a}\right) \quad (1)$$

Where the volume represents the occupied volume by building's material and it is roughly equal to:

$$Volume_{building} = 2.03 \cdot (Area_{footprint} \cdot h_{building})^{0.6373} \quad (2)$$

Therefore, (1) can be rewritten as:

$$scale\ factor = 1.202 + 0.0864 \cdot \left(\frac{a}{b}\right) + 0.0324 \cdot \left(Area_{footprint}^{0.3627} \cdot \frac{h_{building}^{1.3627}}{a}\right) \quad (3)$$

$$h_{building} = \text{total height of the building} \quad (4)$$

$$a, b = \text{respectively are the minor side and major side of the building's footprint} \quad (5)$$

As shown in Figure 21, new simulations for the buildings with one floor and 80 m² are performed to evaluate the variations of debris area increasing the material strength. According to NTC (2008), P1 represents the mechanical parameters used for all collapse simulations in previous analyses, while P2 represents the mechanical parameters used for these new simulations.

P1				P2			
f_m	f_{vk}	E	G	f_m	f_{vk}	E	G
[N/cm ²]	[N/cm ²]	[N/cm ²]	[N/cm ²]	[N/cm ²]	[N/cm ²]	[N/cm ²]	[N/cm ²]
100	2.0	690	230	200	3.5	1020	340

Figure 21. Mechanical properties from P1 to new P2 (NTC2008)

Table 10 reports the comparison between the debris extension adopting P1 parameters and P2 parameters.

Table 10. Compare between Area P1 with Area P2

Ratio	Area P2	Area P1
0.2	229	396
0.3	194	317
0.4	292	445
0.5	247	305
0.6	329	376
0.7	231	253
0.8	337	353
0.9	321	345
1	341	353

In all cases, the results computed in the simulations with the P1 parameters are larger than that with the P2 parameters. The preliminary results seem promising on the reliability of the formula.

3. CONCLUSION

In earthquake affected areas, debris accumulation can be an important problem, as cascading consequence of debris accumulation, the road network can be interrupted. The methodology presented in this research work contributes to this task since is able to provide and assessment of debris generation after a seismic event. The proposed formula could predict whether a road is inaccessible to escape. This approach can be implemented in a more general procedure on a virtual city model, to evaluate the resilience of the road network after collapse of the masonry buildings. It can represent an important input for escape management planning and for waste management planning that will be triggered immediately after a seismic event, allowing rapid removal and relocation of debris in order to facilitate the rescue of victims.

4. ACKNOWLEDGMENTS

The research leading to these results has received funding from the European Research Council under the Grant Agreement n° ERC_IDEAL RESCUE_637842 of the project IDEAL RESCUE-Integrated Design and Control of Sustainable Communities during Emergencies. A special thanks to National Research Institute for Earth Science and Disaster Prevention (NIED) who made available for this research the data obtained from their experimentation.

5. REFERENCES

- Applied Science International, LLC (ASI) (2017), Extreme loading for structures Theoretical Manual
- Autocad 2017, Autodesk Inc., 2017
- Extreme loading for structures 5.0, Applied Science International, LLC (ASI)
- García-Torres, S., Kahhat, R., Santa-Cruz S. (2017). Methodology to characterize and quantify debris generation in residential buildings after seismic events, *Conservation and Recycling*, 117, pp. 151-159.
- Gian Paolo Cimellaro (2016) Urban Resilience for Emergency Response and Recovery, *Springer International Publishing Switzerland*
- Imai, H., Minowa, C., Lanuza, A.G., Penarubia, H.C., Narag, I.C., Soridum, R.U., Okazaki, K., Narafu, T., Hanazato, T., Inoue, H. (2015) A full-scale shaking table test on philippine concrete hollow blocks (Chb) masonry houses, *Journal of Disaster Research*, 10 (1), pp. 113-120.
- Matlab R2017a, The MathWorks, Inc., Natick, Massachusetts, United States.

Rafee N, Karbassi AR, Nouri J, Safari E, Mehrdadi M (2008). Strategic management of municipal debris aftermath of an earthquake. *Int. J. Environ. Res.* 2 (2), 205–214.

Table Curve 3D, SYSTAT Software Inc., 1993-2002

Tanikawa, H., Managi, S., Lwin, C.M., (2014). Estimates of lost material stock of buildings and roads due to the Great East Japan Earthquake and tsunami. *J. Ind. Ecol.* 18 (3), 421–431